Indian Journal of Pure & Applied Physics
Vol. 62, December 2024, pp. 1129-1137
DOI: 10.56042/ijpap.v62i12.13438

Parametric Study of Via Shorting-pin Loaded Novel Shape Miniaturized Monopole Antenna for Body Implantable Applications

Ambresh P A[a]* & Amit Birwal[b]

[a]Department of Applied Electronics, Gulbarga University, Kalaburagi, Karnataka 585 106, India

[b]Electronic Science Department, University of Delhi, South Campus, Delhi 110 021, India

Received 29 August 2024; accepted 6 November 2024

This paper deals with the parametric study of novel monopole antenna with circular ring shape in body-implantable applications. The miniaturized antenna is placed inside skin phantom tissue of human body that has a dimension of 5x5x0.125mm^3. A single wide band is observed for this implantable antenna design with better return loss. The suggested antenna uses a mid-band frequency range of 1520–1693 MHz, ISM band ranging from 433.1–434.8 MHz, and Medical Implanted Communication Service of 402–405MHz. The antenna exhibited compact size and fabricated on RT Duriod 5880 substrate with the property of flexible/ bendable in nature. A significant compact design of the antenna is achieved by using similar dimension of rectangular arms on the circular shape ring patch.The compact dimensions, reduced ground plane, and bandwidths of the suggested antenna are its salient characteristics with the obtained bandwidths are of 500MHz, 550MHz, 650MHz, 585MHz, 690MHz, 652MHz and 740MHz and acceptable gain levels in comparison with other implanted antennas working in the ISM band. The simulated realized gain values are -13.3dBi, -22.1dBi and -18.4dBi respectively.

Keywords: Implantable; Antenna; Size reduction; Return loss; Human body

1 Introduction

Given its many benefits, including cost-effectiveness, decreased bulkiness, compatibility with integrated circuits, and a planar shape, microstrip antennas have been accepted as a distinct entity within the larger area of microwave antennas. Compact microstrip antennas are in elevated demand due to its use in diverse wireless communication environment and mobility of user equipment (UE). In 2G. 3G, 4G, and 5G wireless technologies the use of single or multiband antenna are adopted as per national standards. Literature explores several strategies for miniaturising patch antennas. Various approaches, including slotting[1-5], ground with defective structure (DGS)[6-9], loading of parasitic elements[6,10-15], and others have been utilised. Some antenna structures have drawbacks, such as DGS resulting in complicated designs, parasitic loading, patch with slots having reduction gain and efficiency, and increased antenna area. In case of real-time glucose monitoring applications, a small circularly polarized single fed implantable antenna that operates between 2.40 and 2.48 GHz is built and experimentally proven which uses a complementary split-ring resonator (CSRR) and four C-shaped slots to achieve excellent miniaturization, measuring 8.5 *x* 8.5 *x* 1.27 mm^3. The impedance bandwidth is 12.2% (2.32-2.62 GHz) with a maximum gain of -17 dBi, and the 3 dB axial scaling bandwidth is 2.4% (2.42-2.48 GHz). With S_{11} less than -10dB, the measured impedance bandwidth is 13% (2.31-2.63GHz)[16].

In the industrial, scientific, and medical bands (2.4–2.4835, GHz and 902–928, MHz), a novel tiny dual-band implantable antenna was constructed[17]. The suggested antenna's total volume is restricted to 7 *x* 7.2 *x* 0.2 mm^3 due to the use of 0.1 mm thick Rogers Ultralam liquid crystal polymer base and top layer (εr = 2.9 and tanδ = 0.0025) using the short-circuit pinning method.

In a uniform skin phantom, the employed antenna shows a maximum gain of -28.44 and -25.65 dBi at 928 MHz and 2.45 GHz individually[18]. Through the utilization of slots on the patch plane and the shorting technique, the overall dimensions (including surface area) of the designed antenna can be considerably decreased to 9.8 × 9.8 ×27mm^3 (1. 0.0784λ_0 × 0.0784λ_0 × 0.0102λ_0). In the skin phantom, a -10 dB simulated impedance bandwidth of 21.5 percent and a 3 dB AR bandwidth of 15.8 percent were measured.

*Corresponding author
(E-mail: ambreshpa@redffimail.com)

Both skin and pork mimick gels were used in the experiments, and the measured impedance bandwidths were 25.9 percent and 25.7 percent, respectively[18].

In order to facilitate wireless capsule endoscopy (WCE), the paper suggested[19] an implantable antenna with ultrawide bandwidth that operates in the 401-406 MHz medical device radio communications service band. The suggested antenna performs well in terms of return loss and, consequently, the bandwidth from 284 to 825 MHz is increased, according to the results of the simulation and experiment. This antenna's maximum realized gain at 403 MHz is -31.5 dBi. To meet the specific absorption rate (SAR) requirements outlined in the IEEE standard, the maximum simulated input power is less than or equal to 1.7 mW. These indicate that the proposed antenna is a good candidate for the WCE. Circularly polarized (CP) ground radiation antenna is suggested and investigated for use in biomedical applications [20]. In the suggested antenna, a square ground plane is used. To assess the performance of the antenna, simulations are run using a single-layer tissue model. The antenna's large axial ratio bandwidth, which spans from 2.331 to 2.582 GHz, helps it behave robustly against varying implant depths and biocompatible coating thicknesses. For the 2.4-2.48-GHz Industrial Scientific Medical band, a measured impedance bandwidth of 621 MHz is attained.

In order to serve the Medical Implant Communications Services band (402-405 MHz) and the Industrial, Scientific, and Medical band (2400-2483.5 MHz), a dual-band circular implantable antenna was designed[21] for biomedical applications. The antenna takes up space measuring π × 102 × 2. 54 mm^(797 ÷ 96 mm^). By using vias—openings in the top surface and ground plane—dual band is accomplished using circular patch. The suitability of the design was confirmed by fabricating and measuring the antenna prototype using tissue and pork equivalent fluid models. At 400 MHz and 2.45 GHz, respectively, the maximum gain of the suggested antenna is -33.1 and -14.55 dBi. For each gram of tissue, the specific absorption rate (SAR) was 1. 5 W/kg, and the maximum input power was 6.625 mW.

A metamaterial (MTM)-loaded, compact dual-band circularly polarized antenna system is presented in[22] and is appropriate for a number of biotelemetry applications. The suggested antenna system operates at intermediate frequencies of 915 MHz (902-928 MHz) and 2450 MHz (2400-2480 MHz) in the ISM frequency bands. The compact size (7 mm × 6 mm × 0.254 mm) and dual-band CP capabilities, along with the remarkably high gain values (-17.1 and -9.81 dBi in the lower and upper bands) and slot-less ground plane that reduces backscattered radiation are the main features of the proposed antenna system. In the lower and upper ISM bands, measured impedance bandwidths of 35.8% and 17.8% are obtained.

The design and analysis of tiny implantable conformal chip antennas for biomedical applications where the polyimide substrate material is suggested in this article[23]. A rectangular slot with CPW (coplanar waveguide) feed and three split ring resonators (SRR) make up the radiating element of a monopole rectangular patch antenna. With an impedance bandwidth of 810 MHz and a gain of 2.62 dB, the proposed implantable conformal CPW fed-chip (ICCP) antenna resonates at 2.41 GHz (2.01-2.82 GHz). With the suggested ICCP antenna resonating at 2.60 GHz (2.41-2.81 GHz), an impedance bandwidth of 400 MHz, and a gain of -19.6 dB, an in vitro experiment is taken into consideration in a muscle-imitating phantom gel.

In the research, which spans the MidRadio band (401-406 MHz), ISM (433.1-434.8 MHz, 868-868.6 MHz, 902-928 MHz), and Midfield (1200 MHz) bands, is published[24]. Wireless power transmission (WPT), energy conservation, and biotelemetry are among the uses for these bands. The antenna can be wrapped around the inner wall of the capsule because it is printed on Rogers Ultralum, a flexible material with a thickness of just 0.1 mm. When the fan is folded, its volume is only 48.98 mm^3, compared to 57 mm^3 when it is flat. The proposed conformal antenna in the same rigid phantom operates at 402 MHz with a bandwidth of 27.46 percent, and at 915 MHz and 1200 MHz with a bandwidth of 13.2 percent and 5.42 percent, respectively.

An implantable microantenna system with ultra-wideband capabilities in the 2.4–2.48 GHz industrial, scientific, and medical bands was suggested for biological applications in this study[25]. The substrate on both the top and bottom sides is made of Rogers ULTRALAM, a flexible liquid glass polymer material with Ɛr = 2.9 and loss tangent = 0.0025. The antenna has a large range (1533MHz) and a small size (7*x* 7*x*0.2 mm^3). Higher efficiency and a lower absorption rate (SAR) are features of the suggested antenna.

A triple-band integrated implantable antenna system for various biotelmetry applications that operates in the midband (1824–1980 MHz) and ISM (902–928 MHz and 2400–2483.5 MHz) bands is

described in this paper[26]. The design comprises two implantable devices: a flat type intended for skin implants and a capsule type intended for deep tissue implants. These devices have the following sizes: 647 mm^3 and 425. 6 mm^3. At 7 mm × 6 mm × 0.5 mm, the smallest size suggested, the compact size of the suggested antenna system is 21 mm^3. As a result, the bandwidths measured in saline were 14.7 percent, 24.8 percent in the ISM group, and 13.1 percent in the midband; 8.7 percent, 7.3 percent, and 8.2 percent in the mid band.

A compact antenna designed for LCP integration functioning in the 2.4 GHz ISM band was created in this study[27]. The antenna is designed in a spiral shape to ensure small size, low sensitivity to physical changes, low absorption coefficient (SAR) and small size to reduce construction complexity. The antenna, which is 3 *x* 4 *x* 0.5 mm^3 in size, is built on a high-energy substrate called Rogers RT/duroid 6010. The antenna maintained a good in-band impedance match in ISM band and measured bandwidths are 21.88% and 15.46%. The antenna system's maximum SAR for 1 and 10 g of tissue is 270.28 W/kg and 31.04 W/kg, respectively, and its maximum gain is - 25.95 dBi because of the E-field applied voltage (surface current) on the patch.

This present study deals with the parametric study of novel monopole circular ring shape antenna having the dimension of 5*x*5*x*0.125mm^3 placed inside the skin, muscle tissue of human body used for implantable applications. Section 2 describes the antenna's miniaturized design process. Section 3 provides an explanation of the parametric analysis results, followed by a conclusion and references.

2 Antenna design process

Figure 1 shows a schematic diagram of the proposed compact antenna design of a line-fed ring-shaped circular patch, known as a monopole antenna, without the use of shorting pins. The dimensions of the Substrate are indicated as (*A1 x A2*). The substrate has the circular patch with the slot in the center with diameter indicated as *c* making it to look like circular ring shape fed with stripline with dimension taken as *b* (feed width) and its height is taken as *a.* The back plane of substrate there copper plane acting as ground having hair comb structure indicated with its dimension as given in Table 1. This ground structure is chosen after optimizing the dimension as per the minimal copper structure on ground. The color indication are, yellow portion is the copper and the skyblue color portion is dielectric substrate. The whole simulated prototype is etched on the Rogers RT Duriod 5880 dielectric material with εr = 2.2 and *h* = 0.125mm as its thickness. Final dimension of the design is 5 *x* 5 *x* 0.125mm^3 which is said to compact design and is placed in the skin tissue having dielectric constant εr = 41.6 and loss tangent 0.872 of the considered length and width 50 *x* 50 *x* 0.25mm^3. All the designs are carried out using CST microwave studio simulator.

Later this same design is used but few changes are made for getting the desired performance in the existing design and explained in the different steps as below.

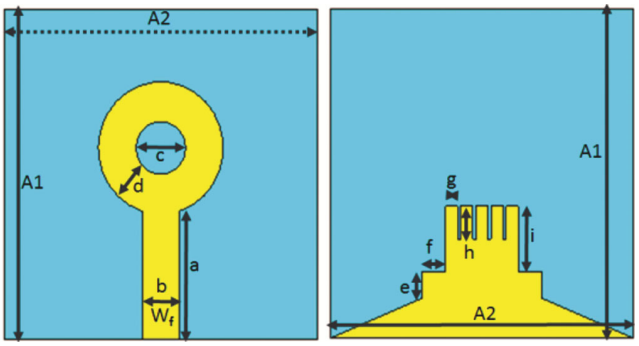

Fig. 1 — Geometry of compact monopole antenna

Tab1e 1 — Optimized values for designed monopole antenna as shown in Figs 1 & 2

Dimension designations	*Values (mm)*	*Dimension designations*	*Values (mm)*	*Dimension designations*	*Values (mm)*
a	1.95	*j*	0.97	*s*	1.28
b (varying)	0.1-0.5	*k*	0.5	*t*	2.82
c	0.8	*l*	0.6	*u*	0.31
d	0.63	*m*	1.75	*A1*	5
e	0.40	*n*	0.5	*A2*	5
f	0.40	*o*	0.44	*Rs*	0.70
g	0.20	*p*	0.7	W_f*(varying)*	0.1-0.5
h	0.50	*q*	0.35	*Shorting pin dia.*	0.4
i	1	*r*	0.70	*Skin tissue*	50*x*50*x*25mm^3

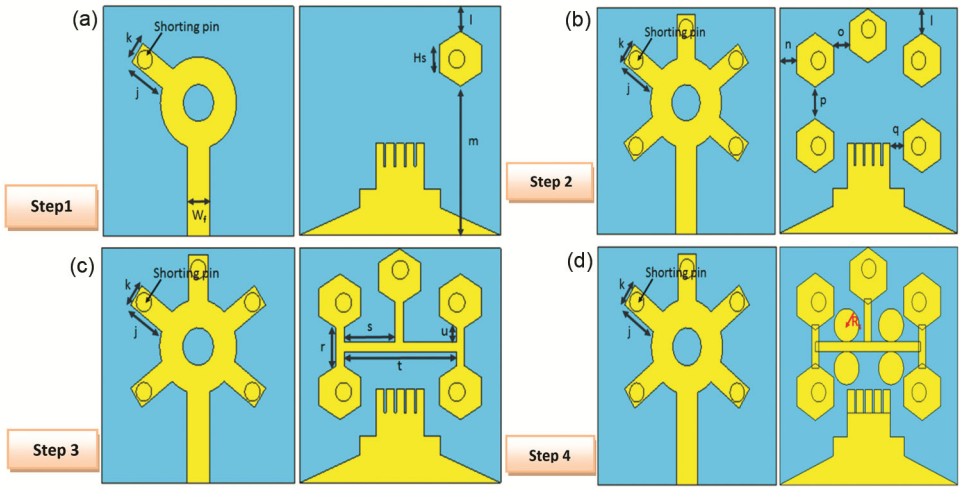

Fig. 2 — Evolution process of novel compact monopole antenna with different optimized parameters

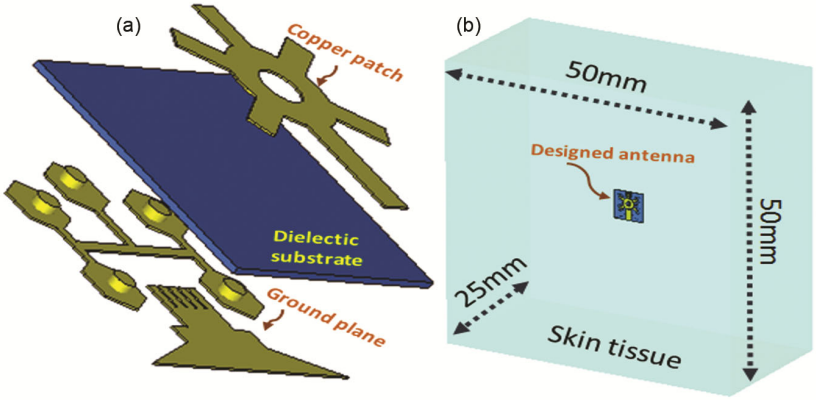

Fig. 3 — Exploded view of the a) deigned antenna and b) placing of it inside the skin phantom tissue.

Step1: In this case, a shown in Fig, 2(a), a single stub in the form of rectangular arm with dimension (*j x k*) is etched towards the left side of the circular ring and the hexagonal patch of placed symmetrical with x-axis in order to get the desired performance characteristics. The extended form of this design is explained in step 2. The dimension details are given in Table 1.

Step 2: In this case, as shown in Fig. 2(b), five single stub in the form of rectangular arm with the same dimension (*j x k*) placed equidistant from each other are sketched towards the right, top and left side on circular ring along with five hexagonal patch of equal side length *Hs* placed on the other side i.e., exactly below the substrate acting as ground plane and all of these are connected with via five shorting pin of 0.4mm are placed symmetrical with x-axis in order to get better performance characteristics. The extended form of this design is explained in step 3. The details of its dimensions are given in Table 1.

Step 3: in this case, a shown in Fig. 2(c), all the five single stub in the form of rectangular arms (stubs) with the same dimension (*j x k*) placed equidistant from each other are etched on the left, top and right side of the circular ring along with five hexagonal ground copper patch of equal side length *Hs* is placed on the other side i.e., exactly below the arms of the patch. The copper patch in form of five hexagons are placed on the ground plane and all of these are connected with via five shorting pin of equal diameter 0.4mm etched symmetrical with x-axis. In order to get still more better performance characteristics, all the five hexagonal copper patch on the ground plane are now connected with three vertical arms of dimension (*r* and *u*) and one horizontal arm of dimension (*s* and *t*) as shown in Table 1. The extended form of this design is explained in step 4. The dimension details are given in Table 1.The view of Fig. 2(c) in the form of exploded picture is shown in Fig. 3(a).

Step 4: in this case, a shown in Fig. 2(d), all the five single stub in the form of rectangular arms with the same dimension (*j x k*) placed equidistant from each other are etched on the right, left and top side on the circular ring along with five hexagonal ground copper patch of equal side length *Hs* placed on the other side i.e., exactly below the arms of the patch on the substrate. The five hexagonal copper type of patch on the ground plane and all of these are connected with via five shorting pin of equal diameter 0.4mm are placed symmetrical with x-axis. In order to get enhanced performance characteristics, all the five hexagonal copper patch on the ground plane are now connected with three vertical arms of dimension (*r* and *u*) and one horizontal arm of dimension (*s* and *t*) as shown in Table 1. A slight modification done in this design is that, four circular small patch with equal dimension (*Rs*) are etched on ground plane and connected to the horizontal arms and the details of its dimensions are given in Table 1. The next section deals of the paper deals with results and its discussions.

The antenna's compact size 5 × 5 × 0.125mm^3 limits its far-field radiation, leading to reduced efficiency and lower gain, especially in lossy, high-dielectric tissue. This impacts communication reliability in deep-tissue environments by attenuating signals more rapidly, which can hinder stable connections with external devices. To mitigate this, designs often focus on optimizing near-field coupling and using lower frequencies that penetrate tissue better, balancing size constraints with acceptable communication ranges for deep-tissue implants.

3 Results and Discussion

This section provides an explanation of the findings for the circular ring monopole implantable antenna. The antennas are prone to frequent interference because they are implanted within the human body. However, the characteristics of the antenna's bandwidth reduce this effect. The proposed design of antenna as shown in Fig. 1 is modeled to operate under ideal circumstances using the CST simulator tool. The simulated bandwidths of 500MHz, 550MHz, 650MHz, 585MHz, 690MHz, 652MHz and 740MHz which covers MICS, ISM bands respectively. The proposed antenna has a better bandwidth and a higher reflection coefficient as shown in Fig. 4. The antenna is first submerged inside skin phantom tissue having dimension 50*x*50*x*25mm^3

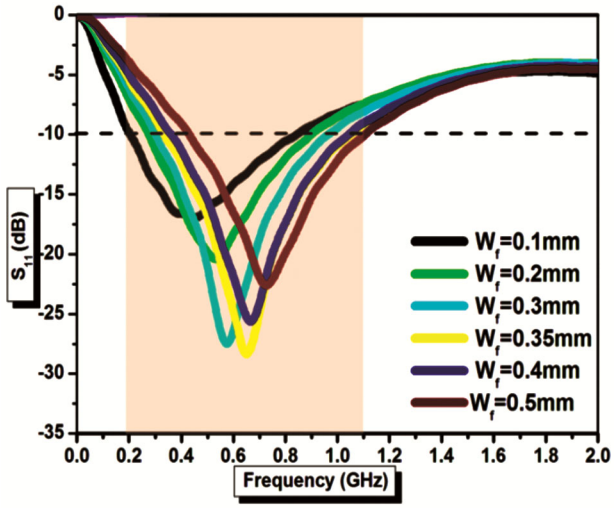

Fig. 4 — Observed S_{11} for Compact novel monopole antenna for different values of W_f

as seen in Fig. 3. Because of variations in feed deign of antenna, the $|S_{11}|$ responsiveness of the antenna with good matching response in MICS and ISM band, a bandwidth of 550 MHz and 652MHz are obtained.

Figure 4 displays the observed return loss (S_{11}) of the designed monopole antenna having circular ring patch, which attained a wide bandwidth of 500MHz (for W_f = 0.1mm) and resonates at 415MHz with a return loss of -17.5 dB, is appropriate for ISM band applications. Fig. 4 illustrates (in black curve) covering the frequency range from 0.2GHz to 0.7GHz, with two distinct frequencies, having return losses less than -10dB respectively, and the obtained bandwidth still can be improved by changing W_f (width of feed). The ground plane length and width are not varied in several iterations to optimize the results displayed. In addition, it can be seen that the parametric analysis is also performed by changing the feed width (W_f). By connecting a short pin between the patch and the ground plane, the antenna is designed to resonate at low-band that further improves its return loss to provide the wide bandwidth.

3.1 Parametric study1: Changing the feed width

As depicted from the Fig. 4, five different sets of S_{11} are obtained with improved bandwidth and return loss. With the feed dimension W_f = 0.2 mm, the antenna resonated from 0.3GHz to 0.85GHz(in green curve) with center frequency of 0.55GHz with return loss of 21dB. The observed improved bandwidth is 550MHz.

By increasing the W_f = 0.3 mm, the antenna here resonated from 0.29GHz to 0.95GHz (in blue curve) with center frequency of 0.585GHz with return loss of 27dB. The observed improved bandwidth is 650MHz. With an increase in the W_f to 0.35 mm, the antenna here resonated from 0.35MHz to 1GHz (in yellow curve) with center frequency of 0.65GHz with return loss of 28dB. The observed improved bandwidth is 652MHz. When the feed width is further increased to W_f= 0.4 mm, the antenna resonated from 0.37MHz to 1.05GHz with center frequency of 0.66MHz with return loss of 26dB. The observed improved bandwidth is 654MHz. Finally, when the feed width is further increased to W_f= 0.5 mm,the antenna resonated from 0.41MHz to 1.1GHz with center frequency of 0.71GHz with return loss of 23dB. The observed improved bandwidth is 690MHz.

3.2 Parametric study 2: as per the design evolution

As depicted in the Fig. 5, it illustrates the observed S_{11} curve for the different design evolution process for the compact monopole antenna. For the initial design (in step 1) as shown in Fig. 2(a), the S_{11} curve was found to be slightly moving towards the -10dB line with negligible bandwidth and it can be neglected. For the second design (for step 2), the return loss curve of this antenna design with five rectangular arms and five hexagonal ground copper connected with shorting pins, the S_{11} curve is now crossing the -10dB line with frequency ranging from 0.49GHz to 0.9GHz with the bandwidth of 410MHz having return loss of -12dB.

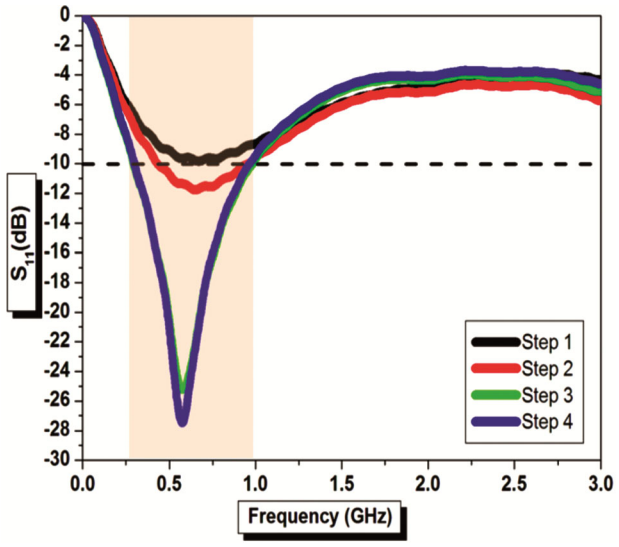

Fig. 5 — Observed S_{11} of designed antenna at various evolution process

For the third design (for step 3), the return loss curve of this antenna design with five rectangular arms, five hexagonal ground copper connected with shorting pins and all the hexagons are now connected with vertical and horizontal arms on the ground plane. In this case, the S_{11} curve has a better -10dB return loss curve line with frequency ranging from 0.49GHz to 0.91GHz achieving bandwidth of 411MHz with improved return loss of -25dB. For the last design (for step 4), the return loss curve of this antenna design with five rectangular arms, five hexagonal ground copper connected with shorting pins and all the ground plane hexagon patches connected with vertical and horizontal arms with four circular patches connected to these arms on ground plane, in this case, the S_{11} curve has a still more better -10dB return loss curve line with frequency ranging from 0.30GHz to 0.99GHz with the attained improved bandwidth of 690 MHz having improved return loss of -28dB as shown in Fig. 4. Hence, step 4 antenna design yields better return loss with improved bandwidth up to 690MHz at 0.52GHz resonance.

3.3 Parametric study3: changing the hexagonal side length

From the Fig. 6, it can be noticed that, three different analysis has been carried out for the different values of hexagonal side length (*Hs*) ranging its dimensions from 0.35 to 0.9 mm. With initial change in hexagonal side length (*Hs*) of 0.35 mm and retaining all the other dimensions of antenna, thus the antenna resonated at center frequency 0.62GHz (with its band ranging from 0.35GHz to 1.07GHz: as in black curve) having return loss of -21.5dB attaining the bandwidth of 740MHz.

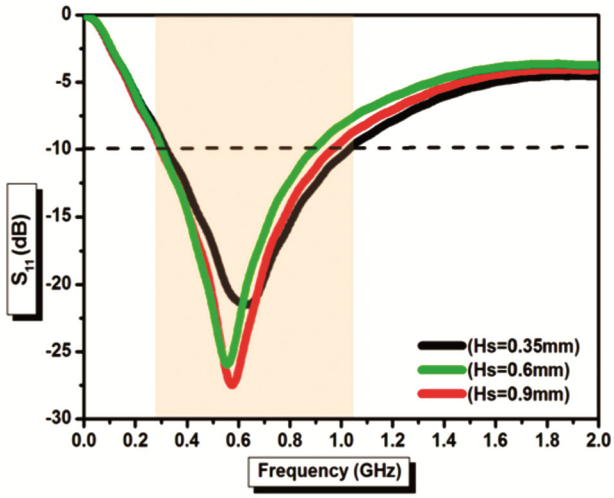

Fig. 6 — Designed antenna S_{11} for different values of *Hs*

Table 2 — A comparison of the proposed antenna with other reported antennas

Ref	Size	Freq (MHz)	Gain
[17]	7×7.2×0.2 mm^3	928	−28.44 dBi
[18]	9.8 × 9.8 × 1.27 mm^3	2400	-32.8 to -35.7 dBi
[19]	15×15.2 mm^2	401-406	-31.5 dBi
[20]	10.4 × 10.4 × 0.508 mm^3	2400	-21.1 dBic
[21]	π × 10 2 × 2.54 mm^3	402-405 and 2400-2483.5	-33.1 and -14.55 dBi
[22]	7 mm × 6 × 0.254 mm	915 and 2450	-17.1 and -9.81 dBi
[24]	19 mm × 15 mm × 0.2 mm	402, 915 and 1200	-30.8, -19.7 and 18.7 dBi
[26]	7 mm × 6 mm × 0.5 mm	902-928, 1824-1980 and 2400-2483.5	-26.4, -23, -20.4
This work	5×5×0.125mm^3	415, 500, 615	-13.3, -22.1 and -18.4dBi

In the second case, the hexagonal side length (*Hs*) is changed to 0.6 mm, making the antenna resonate at center frequency 0.58GHz and its frequency band is now ranging from 0.3GHz to 0.85GHz (for green curve) having bandwidth of 550MHz with return loss of -26.5dB. Lastly, for the third case, the change of hexagonal side length (*Hs*) up to 0.9 mm, makes the antenna resonate at center frequency 0.595GHz with its resonance band ranging from 0.29GHz to 0.95GHz (for red curve) attaining the bandwidth of 660MHz with return loss of -27.5dB as given in Table 2. Therefore, by adjusting Hs, the first case design, with *Hs* = 0.35mm, achieves higher performance in terms of bandwidth and with HS=0.9mm the antenna has attained better dip in return loss.

3.4 Parametric study 4: changing the ground circular patch radius

Figure 7 illustrates how the return loss and bandwidth are examined for various values of the ground plane circular patch radius (Rs), ranging from 0.1 to 0.35mm. With the initial value of *Rs* = 0.1 mm, the antenna resonated for the band ranging from 0.3GHz to 0.94GHz (as shown in black curve) with center frequency at 0.585GHz having bandwidth (BW) of 640 MHz and RL = -26.5dB. With change in radius of circular shape *Rs* to 0.2mm, the antenna now resonates for the band ranging from 0.33GHz to 0.94GHz (as shown in red curve) having center frequency at 0.59GHz with BW of 610 MHz and RL = -24.5. Lastly with the value raised to *Rs* = 0.35 mm, the antenna resonated for the frequency band ranging from 0.29GHz to 0.94GHz (as shown in green curve) with center frequency at 0.57GHz having bandwidth of 620 MHz having deeper RL up to -32dB as given in Table 2. Hence, with circular patch radius *Rs* = 0.1 mm on the ground plane has obtained the better bandwidth with *Rs*=0.35mm the antenna has attained lowered the resonant band with better dip in return loss upto -32dB as shown in Fig. 7.

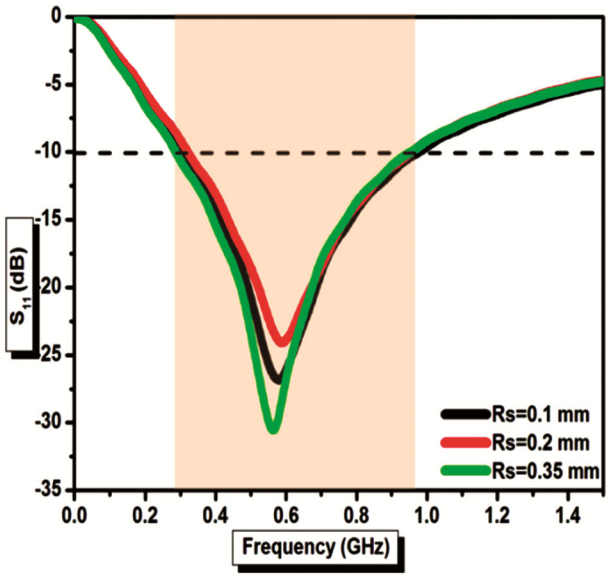

Fig. 7 — Designed antenna$S_{11}$for different values of *Rs*

Other implantable antennas in the ISM band have attained the bandwidth upto 410 MHz. At resonant frequencies of 0.415GHz, 0.50GHz and 0.615GHz, the simulated gains are found to be -13.3dBi, -22.1dBi and -18.4dBi respectively for the proposed antenna. As shown in Fig. 8, it is quite evident that, the whole novel patch design with copper creates single resonance along with feed and ground plane and hence single wide band characteristics is obtained as final outcome desirable for ISM band applications as shown in Table 2.

Figure 9 displays the radiation patterns at various frequency bands for the designed antenna.All the reading shows the better co polar and minimal cross polar readings for 0.415GHz, 0.50GHz and 0.615GHz.The pattern are observed to be omni-directional in nature in all the cases. The simulated gains at these frequencies are found to be -13.3dBi, -22.1dBi and -18.4dBi respectively. Integrating the proposed monopole antenna into real-world

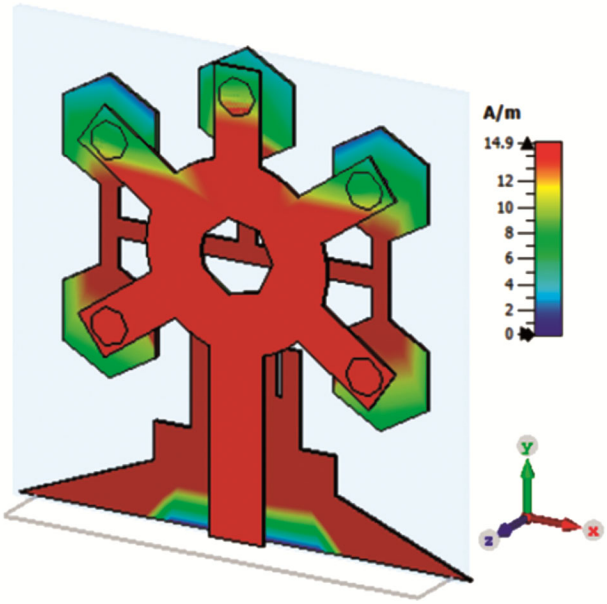

Fig. 8. — Surface current distribution of Compact monopole antenna

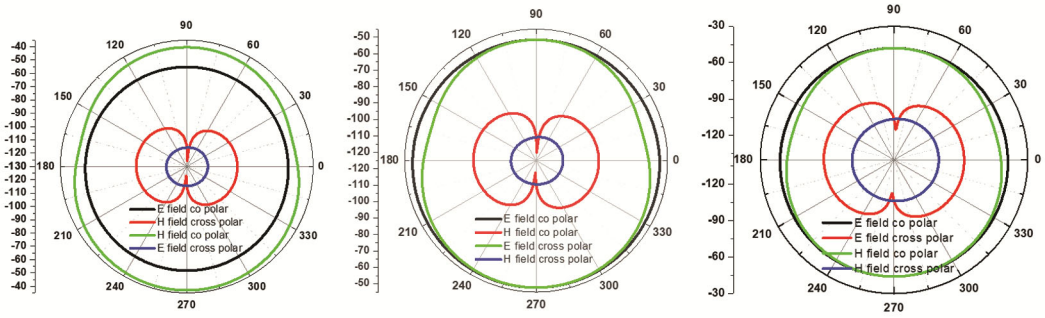

Fig. 9 — Radiation patterns at 0.4GHz, 0.5GHz and 0.6GHz

biomedical devices presents several potential challenges, mainly concerning the performance, biocompatibility, safety, and stability of the antenna within human tissue. Since the antenna is to be implanted, it must be biocompatible to avoid tissue irritation or adverse reactions. The substrate, RT Duriod 5880, while flexible, may require a biocompatible coating (such as Parylene or silicone) to ensure safety for long-term implantation. Human tissue absorbs electromagnetic waves, especially at high frequencies, which can significantly reduce antenna performance and signal strength. As observed, the realized gain values are relatively low, with negative dBi levels (e.g., -13.3dBi, -22.1dBi, -18.4dBi). To counter this, designing for optimized positioning within the body, closer to the skin or in areas with less dense tissue, could improve signal strength.A comparasion of the proposed antenna with other reported antenna is presented in Table 2. It is found that the proposed antenna is compact in size and offers a high gain compared to other reported antennas.

4 Conclusion

In this paper, various parametric analysis studies of compact monopole antenna design are carried out with the changes in thefeed width, study carried out as per the design evolution, with the changes in the hexagonal side length and lastly changing the ground circular patch radius. The suggested antenna is made of RT Duriod 5880 substrate, which is flexible and bendable and has a small size. The antenna's notable compact design is accomplished by the use of rectangular arms with comparable dimensions on a circular ring patch. The designed antenna is flexible and obtained the band widths of 500MHz, 550MHz, 650MHz, 585MHz, 690MHz, 652MHz and 740MHz within the desired frequency range from 0.3 to 1.1 GHz and good gain

values in comparison to existing implantable antennas at ISM band are the main characteristics. Fabricating this flexible antenna with RT Duriod 5880 poses challenges in precision patterning and maintaining material integrity during bending. Techniques like photo-lithography for accurate etching and laser machining for fine details ensure precision. Quality control with automated testing and robust encapsulation would maintain consistent performance in mass production. As a future scope, the study can be evaluated with different dielectric substrates to get still more enhanced characteristics.

Acknowledgment

The authors gratefully acknowledge to Department of Electronic Science, University of Delhi, South Campus, India for providing opportunity to use the CST software for the simulation.

Conflicts of Interest

We the authors hereby declare that there is no conflict of interest.

References

1 Prasad K D, Ali T & Biradar R C, *Inform Commun Technol (RTEICT)*, (2017) 820.
2 Parikh R, Singh B, 4th *Int Conf Comput Commun Control Automat*, ICCUBEA, (2018) 1.
3 Chang D, Liu J, Zeng B, Wu C, Liu C & Operations A D, *Compact Double-Ring Slot Antenna with Ring-Fed for Multiband Applications*, (2006) 2.
4 Abolade J O, Konditi D B O & Dharmadhikary V M, *Heliyon*, 7 (2021) e06247.
5 Abolade J O, Konditi D B O & Dharmadhikary V M, *J Eng*, (2021) 1.
6 Das T K, Dwivedy B & Behera S K, *AEU - Int J Electron Commun*, 118 (2020) 153130.
7 Hussain R, Khan M U & Sharawi M S, *IEEE Antenn Wireless Propag Lett*, 17 (2018) 142.
8 Yadav A, Goyal S, Agrawal T & Yadav R P, *Int Conf Recent Adv Innovat Eng*, ICRAIE, (2016) 1.
9 Mark R, Mishra N, Mandal K, Sarkar P P & Das S, *AEU - Int J Electron Commun*, 94 (2018) 42.
10 Chen W, Yao Y, Yu J, Liu X & Chen X, *IEEE Int Wirel Symp*, (2015) 1.
11 Rezvani M & Zehforoosh Y, *AEU - Int J Electron Commun*, 93 (2018) 277.
12 Liu H, Lu B & Li L, *Int J Antenna Propag*, (2015) 1.
13 Yan Y, Jiao Y & Zhang W, 12th *Int Symp Antennas, Propag EM Theory*, ISAPE, (2018) 1.
14 Sim C, Yeh C & Lin H, *Int Symp Antennas Propag Conf Proc*, (2014) 469.
15 Li Y & Chu Q, 14th *Eur Conf Antennas Propag*, (2020) 1.
16 Liu X Y, Wu Z T, Fan Y & Tentzeris E M, *IEEE Antennas Wirel Propag Lett*, 16 (2017) 577.
17 Faisal F & Yoo H, *IEEE Trans Antennas Propag*, 67 (2019) 774.
18 Xia Z, *et al*., *IEEE Trans Antennas Propag*, 68 (2020) 2399.
19 Wang J, Leach M, Lim E G, Wang Z, Pei R & Huang Y, *IEEE Trans Antennas Propag*, 17 (2018) 1153.
20 Lei W, Chu H & Guo Y, *IEEE Trans Antennas Propag*, 64 (2016) 2535.
21 Ganeshwaran N, Jeyaprakash J K, Alsath M G N & Sathyanarayanan V, *IEEE Antennas Wirel Propag Lett*, 19 (2020) 119.
22 Zada M, Shah I A & Yoo H, *IEEE Trans Antennas Propag*, 68 (2020) 1140.
23 Ketavath K N, Gopi D & Rani S S, *IEEE Access*, 7 (2019) 43547.
24 Yousaf M, *et al*., *IEEE Access*, 8 (2017) 157617.
25 Yousaf M, *et al*., *IEEE Access*, 9 (2021) 40086.
26 Zada M & Yoo H, *IEEE Trans Antennas Propag*, 66 (2018) 7378.
27 Zada M, Shah I A, Basir A & Yoo H, *IEEE Trans Antennas Propag*, 69 (2012) 1152.